

Beam Fragmentation in Heavy Ion Collisions with Realistic Nuclear Configurations

M. Alvioli, M. Strikman

104 Davey Lab, The Pennsylvania State University, University Park, PA 16803, USA

(Dated: February 26, 2019)

We develop a new approach to production of the spectator nucleons in the heavy ion collisions. The energy transfer to the spectator system is calculated using the Monte Carlo based on the updated version of our generator of configurations in colliding nuclei which includes a realistic account of short-range correlations in nuclei. The transferred energy distributions are calculated within the framework of the Glauber multiple scattering theory, taking into account all the individual inelastic and elastic collisions using an independent realistic calculation of the potential energy contribution of each of the nucleon-nucleon pairs to the total potential. We show that the dominant mechanism of the energy transfer is tearing apart pairs of nucleons with the major contribution coming from the short-range correlations. We calculate the momentum distribution of the emitted nucleons which is strongly affected by short range correlations including its dependence on the azimuthal angle. In particular, we predict a strong angular asymmetry along the direction of the impact parameter \mathbf{b} , providing a unique opportunity to determine the direction of \mathbf{b} . Also, we predict a strong dependence of the shape of the nucleon momentum distribution on the centrality of the nucleus-nucleus collision.

PACS numbers: 25.75.-q, 25.75.Dw, 24.10.-i, 21.60.Ka

I. INTRODUCTION

In this paper we start a program of studies of the nuclear fragmentation in relativistic heavy ion collisions using as a starting point an event generator of the nucleon configurations in nuclei which correctly reproduces short-range correlations between the nucleons.

Most of the recent experimental and theoretical studies of the relativistic heavy ion collisions were focused on the production of hadrons in the central rapidities. Fragmentation of nuclei in these collisions was used only as a supplementary trigger for centrality. At the same time experiments at RHIC have demonstrated that it is possible to determine on the event by event basis impact parameter and reaction plane of the collision. (there is obviously some inherent uncertainty related to the fluctuations of the observables for collisions at a given impact parameter). This opens new opportunities for studies of the nuclear fragmentation which have a long history, see for example Ref. [1] and references therein.

Another motivation is the recent direct observation of Short Range Correlations (SRC) [2–5] in the nuclear decays initiated by hard removal of the nucleon from the nucleus. When combined with the scaling of the ratios in $x > 1$ (e, e') nuclear reactions, it demonstrates the important role played by SRC in nuclear structure, for a recent review see [6]. This calls for description of heavy ion collisions using a realistic configurations of nucleons in nuclei going beyond the commonly used collection of nucleons randomly distributed in the nuclear volume.

A first step towards the inclusion of SRC in nuclear configurations was done in Ref. [7] considering the implementation of central correlation functions within a Metropolis method. This overcomes the problem of distortion of single particle density when configurations with nucleons at short distance are simply discarded, and also generates configurations whose pair distribution function

is close enough to the realistic one; in particular, it vanishes when the two nucleons separation approaches zero.

In [7] the inclusion of correlations in nuclear configurations was shown to have significant effects on fluctuations of the average number collisions in NA scattering; the authors of Ref. [8, 9] confirmed our findings about fluctuations in NA as well as AA collisions using our central-correlated configurations [10] within their Monte Carlo (MC) simulations. In this work we have implemented a second step, taking into account spin and isospin dependence in the generation of configurations, which in principle enables us to implement state dependent correlations; this procedure is discussed in Sect. II.

In this paper we apply an improved MC method for discussing correlation effects in AA collisions at the energies of the CERN NA49 experiment [11], and also using results from the LBL experiment of Ref. [12]. We try to address the question of the determination of centrality in a given collision, which in MC generators is usually extracted from the correlation between the observed charged particle multiplicity and the calculated number of participant nucleons in the AA collision. This usually leads to large uncertainties and the impact parameter is usually known in large bins and very central collisions are difficult to identify. We propose in this work that one can obtain additional information about the centrality of a collision, based on the detailed balance of energy transferred in the collision at given impact parameter and on the emission of high-momentum nucleons originating from SRC pair in nuclei. In addition, the angular asymmetry for emission of nucleons allows to resolve the sign ambiguity of the direction of impact parameter \mathbf{b} as the usual procedures determine only $|\mathbf{b}|$.

We introduce a new model for the description of the emission mechanism of spectator nucleons in ultra-high energy heavy ion collisions. In this limit, in the rest frame of one of the nuclei, the projectile is strongly Lorentz con-

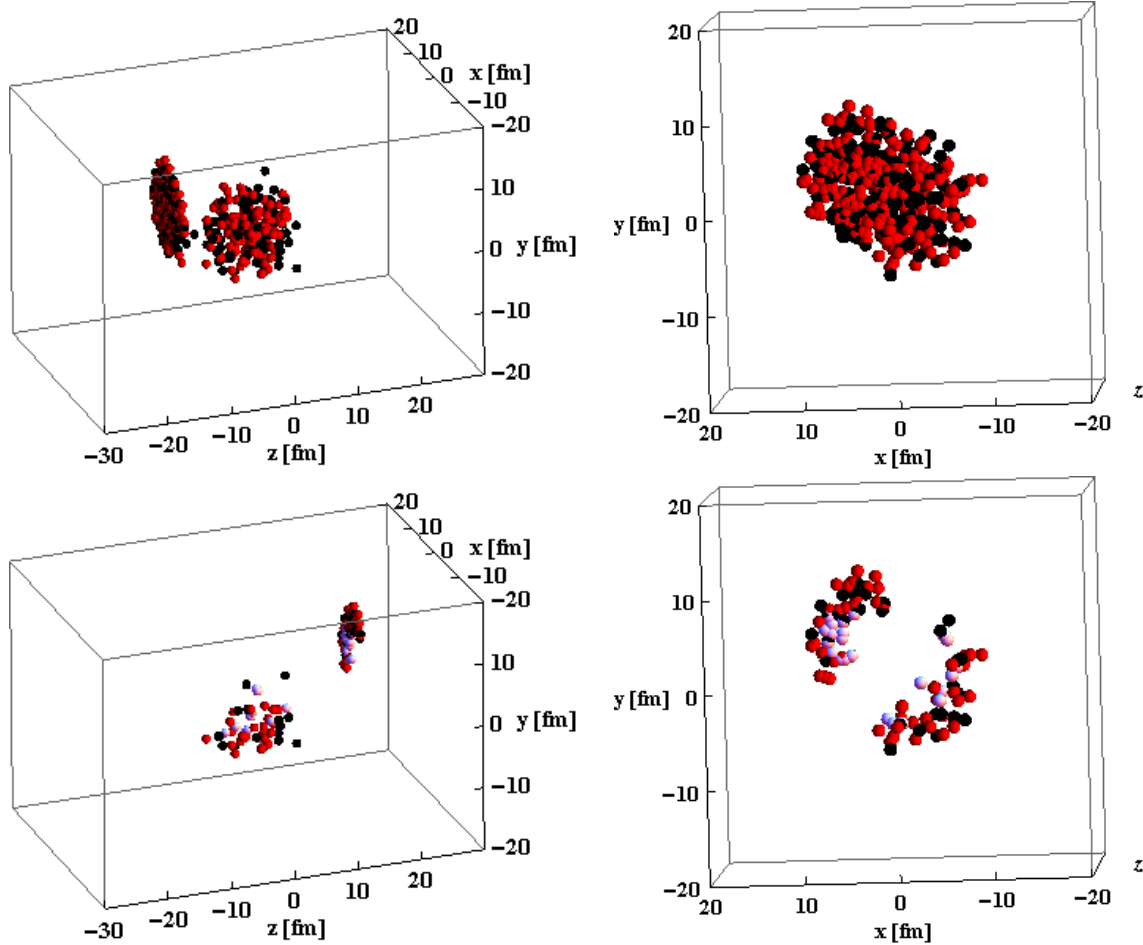


FIG. 1: (Color Online) Sketch of a $Pb - Pb$ collision in the target rest frame, at impact parameter $b = 5$ fm oriented at 45 degrees with respect to the x and y axes; the projectile moves along the z axis. *Left*: view along the beam line; *right*: view from behind; *top panels*: before interaction; *bottom panels*: after interaction; the inelastically interacting nucleons have been removed from the figure. Black and red spheres represent protons and neutron, respectively, while the white ones are active nucleons (see text). The dimension of the spheres are taken as the rms charge radius of the proton. Animations are available at the URL in Ref. [10] along with the configurations used for the colliding nuclei.

tracted to the longitudinal size of the order $\leq 1/\mu$ where μ is a soft strong interaction scale $\leq m_\rho$. As a result, the collision can be considered as the propagation of a “pancake” moving with the speed of light which consequently removes nucleons from the target along its path; the situation is depicted in Fig. 1. It is worth emphasizing that dynamics of nuclear fragmentation at low energies is very different - energy transfers to individual nucleons is small as compared to the scale of energies in short-range correlations, the relative speeds of nuclei are small - far from the picture of a thin pancaked nucleus going through the target nucleus we can employ in the ultrarelativistic collisions; for a review of models of fragmentation at low energies see Ref. [13]. The spectator system emerging from the target is left in an unknown excited state. At the first stage the destruction of the potentials between the pairs (triplets) of nearby nucleons, one of which is hit and another belongs to the spectator system, release energy on the layer of nucleons adjacent to the removed

portion of the nucleus. This energy comes from the work performed by destruction of the potential energy (bonds) associated with the position of these nucleons in the initial wave function, and it can be readily converted into kinetic energy. As a result, they can be emitted into free space in the direction of the removed nucleons, or propagate into the spectator system and undergo attenuation. The remaining available potential energy goes into excitation of the spectator system and it can be released at a later stage by standard nucleon evaporation and decay.

Realistic calculations of the fractions of total potential energy due to the different pp and pn pairs in nuclei based on the method of Ref. [14] shows that, while the two contributions are proportional to the corresponding number of pairs, the inclusion of correlation drastically changes these fractions, bringing the pn pairs to carry about 85% of the total potential energy, as discussed in detail in Sect. III.

Our model for the first stage, which immediately fol-

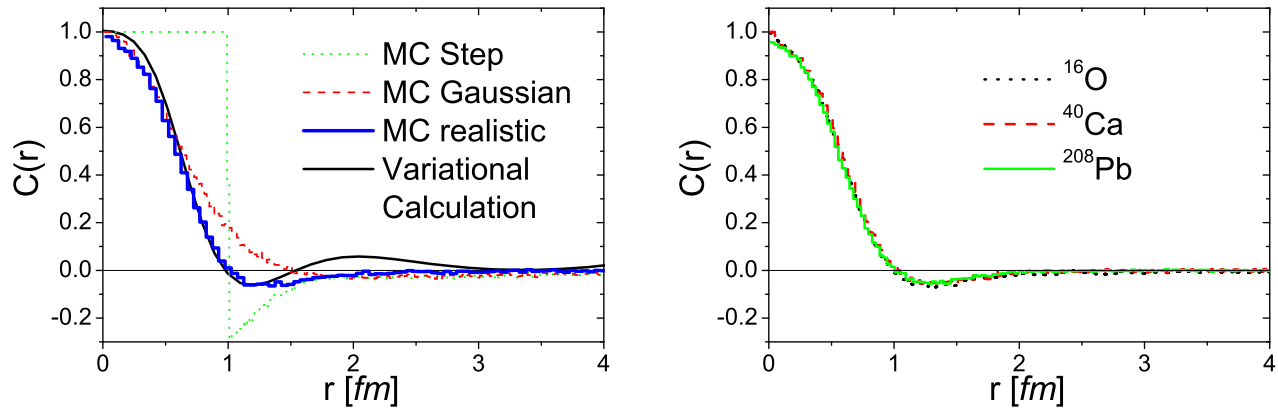


FIG. 2: (Color Online) The pair distribution function of defined in Eq. (2). *Left panel:* $C(r)$ of ^{16}O , obtained with MC within various approximations for the nucleon-nucleon correlation functions, compared with the variational calculation of Ref. [14]. *Right panel:* $C(r)$ calculated with the updated nucleon configurations of the present work for ^{16}O , ^{40}Ca and ^{208}Pb nuclei.

lows the initial removal of a certain number of nucleons, is based on the Glauber description of the collision, which allows an impact-parameter dependent description and which takes into account the basic features of realistic calculations of short range correlations in the ground state of nuclei [14]. As a matter of fact, the Glauber model is the framework for MC codes such as HIJING [15] for the simulation of nucleus-nucleus collisions. The number of participants is defined as the nucleons which interacted inelastically at least once in the AA collision, and spectators are the nucleons which didn't interact. They are determined within the Glauber approximation and the simulation of the whole process is performed assuming that these quantities can be calculated starting from random nucleons distributed according to a given probability density for the nucleus profile. The aim of our contribution is to carry out the calculations outlined above implementing realistic configurations which take into account nucleon-nucleon correlations.

In Sect. IV we describe the algorithm for the selection of correlated nucleons among the nucleons close to the collision surface. Moreover, we outline the procedure we have used to produce the soft, low momentum part of the distribution from heating and evaporation of the residual system, as well as how we model the production, propagation through the residual system and emission of correlated, high momentum nucleons. Elastic scatterings between primary nucleons and attenuation of the emitted nucleons by the spectator system are described in Sect. V.

The procedure outlined above is applied in Sect. VI for the calculation of the momentum distribution of nucleons produced by decay of the excited nuclear system and by emission from the collision surface. An additional mechanism of nucleon production due to elastic scattering of nucleons near the surface of the collision is also described in this Section.

In section VII we discuss a novel feature of the proposed mechanism of nucleus fragmentation - the strong angular dependence of the emission. It is due to a large contribution of the emission from the inner surface generated by removal of a fraction of nucleons due to the collision, which is strongly dependent on the geometry of the process. We expect an azimuthal asymmetry which can be exploited to determine the centrality of a given collision event and also resolve the sign ambiguity of the impact parameter vector.

In Section VIII we discuss a comparison with previous models. Particularly interesting is the analysis of Ref. [1], in which the abrasion-ablation model is used to define the participant-spectator mechanism and the subsequent spectator system decay, and an estimate of the excitation energy per spectator nucleons is performed. We find that our results for the average characteristics of the nucleon emission which were considered in the model are close to the result of Ref. [1] where certain inputs from the data were used.

II. GENERAL DEFINITIONS AND METHOD

The inclusion of central correlations in nuclear configurations can be achieved within a Monte Carlo Metropolis method by using as a probability function the square of the wave function of the system taken in the following form:

$$\psi_0(\mathbf{r}_1, \dots, \mathbf{r}_A) = \hat{F} \phi_0(\mathbf{r}_1, \dots, \mathbf{r}_A), \quad (1)$$

where $\phi_0(\mathbf{r}_1, \dots, \mathbf{r}_A)$ is a Slater determinant of single particle densities and the correlation operator \hat{F} can in principle include the dependence upon all the state-dependent operators contained in realistic nucleon-nucleon potentials; in Ref. [7] a simple product of central correlation functions was considered, $\hat{F} \equiv F =$

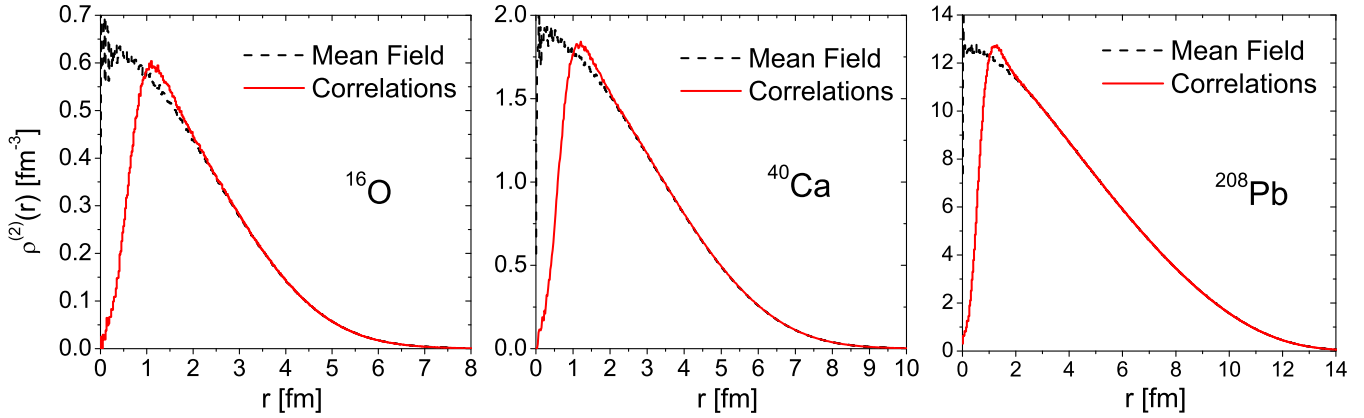


FIG. 3: (Color Online) The full (NN) state dependent two-body density matrix defined in Eq. (5) calculated for ^{16}O (left), ^{40}Ca (center) and ^{208}Pb (right). The comparison of the central correlated results (dots) and the full correlation results (full lines) for the six $\hat{O}_{12}^{(n)}$ operators of Eq. (6) is shown in the various panels. The curves are normalized to $4\pi \int r dr \rho^{(2)}(r) = A(A-1)/2$.

$\prod_{i<j}^A f(r_{ij})$. The calculation which includes the full product $\hat{F} = \prod_{i<j}^A \hat{f}(r_{ij})$ with \hat{f} the state-dependent correlation functions, is a formidable task; instead, one can consider an expansion of that product whose first term contains correlation links of the particle under investigation in the Metropolis search with a second particle only, disregarding correlation links between the second particle and the others. The subsequent terms which include such third- and higher-order correlations, namely three-body clusters linked by spin and isospin dependent two-body correlations, as well as genuine three-body correlations, will be neglected in the present work. At the same time the central correlations will be retained to all orders. This procedure is dictated by the enormous computing power needed by a higher-order calculation and justified by the fact that realistic calculations based on the cluster expansion technique show that higher-order calculations, essential for the accurate determination of quantities such as binding energy and momentum distributions, provides corrections to the bulk properties of the quantities of relevance, namely diagonal one- and radial two-body densities, which are small as compared to the accuracy needed by our study. Instead, we will make use of realistic results obtained within the cluster expansion method ([14, 16]) when applicable. The pair distribution function

$$C(r) = 1 - \rho_C^{(2)}(r)/\rho_U^{(2)}(r), \quad (2)$$

with $\rho_C^{(2)}$ and $\rho_U^{(2)}$ being the Correlated and Uncorrelated two-body radial density, respectively, is presented in Fig. 2; we have shown, in addition to the results of Ref. [7] obtained in MC with step (theta function) and gaussian nucleon-nucleon correlation functions, the result obtained with the improved configurations described in this Section and compared with the variational calculation from Ref. [14]. It can be seen that a much better

behavior is found using the improved configurations, as compared with the realistic result; the second panel of the figure shows $C(r)$ for other nuclei.

The description of the nucleus-nucleus collisions can be made at high energies within the Glauber multiple scattering theory. Within this description, nucleons are frozen in their position during the interaction, which is supposed to be instantaneous; for a given impact parameter of the colliding nuclei, the impact parameter $\mathbf{b}_{ij} = \mathbf{b}_i - \mathbf{b}_j$ of the i -th projectile and j -th target nucleons are considered, and their (inelastic) interaction is evaluated using the Glauber formula:

$$P_{in}(b) = 1 - (1 - \Gamma(\mathbf{b}_i - \mathbf{b}_j))^2, \quad (3)$$

on an Monte Carlo event-by-event basis; the $\Gamma(b_{ij}) = \sigma_{NN}^{tot} \exp(-b_{ij}^2/2B)/4\pi B$ function in Eq. (3) is the usual nucleon-nucleon elastic profile function, in which we used the parameters $\sigma_{NN}^{tot} = 39 \text{ mb}$ and $B = 13.59 \text{ GeV}^2$, corresponding to NA49 energy; the calculations can be repeated for energies other than this particular one, as long as the high-energy Glauber approximation is applicable (we neglect here inelastic shadowing corrections which arise in the Gribov-Glauber approximation - these effects primarily affect interactions far from the interaction surface). We also give results for the energies of RHIC and LHC. For illustration purposes, we show in Fig. 1 the spectator nucleons after a $Pb-Pb$ collision, for two particular projectile-target configurations. The figure shows, in addition to protons and neutrons (respectively black and red), nucleons which before the event were correlated with an interacting nucleon; these are shown explicitly in white; correlated pairs were identified checking their relative distance and choosing correlated nucleons on the basis of the potential energy they can gain by removal of neighboring nucleons, as described in the next Sections.

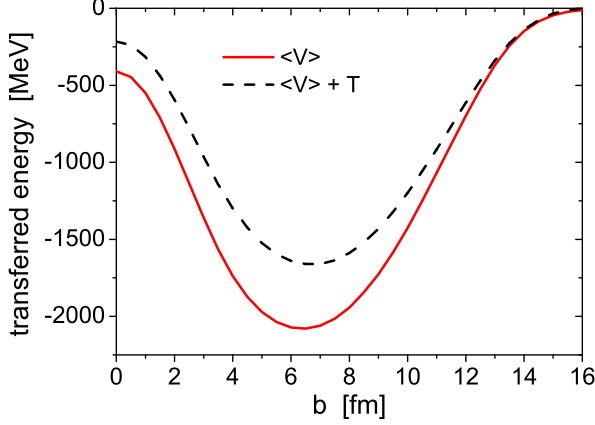


FIG. 4: (Color Online) Transferred energy in $Pb - Pb$ collisions at $P_{Lab} = 160$ GeV, calculated within our model at different impact parameters. *Solid line*: potential energy due to removing of nucleons with no other effects taken into account; *dashed line*: transferred energy after i) subtraction of kinetic energy of emitted high-momentum nucleons ii) emission of soft nucleons from the interaction surface iii) extra energy gained from absorbed elastically scattered nucleons and absorbed by the spectator system.

III. POTENTIAL ENERGY CALCULATION

One of the purposes of this work is to evaluate the energy transferred in the collision of two heavy nuclei. To this end, we considered the method of cluster expansion of Refs. [14], [16], and found that i) the inclusion of correlations into the potential energy calculation bring the fraction of total potential energy $\langle V \rangle_{NN}$ due to pn pairs to about 85%, due to the existence of tensor interactions in the nucleon-nucleon potential; ii) the state-dependent radial two-body densities $\rho_n^{(2)}(r)$ calculated in Refs. [14], [16] can be incorporated in our Monte Carlo code to check what fraction of the total energy is transferred during the event and what is the contribution that can be ascribed to SRCs.

The potential energy contribution to the ground state energy can be calculated according to

$$\langle V \rangle = \frac{A(A-1)}{2} \sum_{n=1}^6 \int d\mathbf{R} d\mathbf{r}_{12} \rho_n^{(2)}(\mathbf{R}, \mathbf{r}_{12}) v^{(n)}(r_{12}), \quad (4)$$

where $\mathbf{R} = (\mathbf{r}_1 + \mathbf{r}_2)/2$, $\mathbf{r}_{12} = \mathbf{r}_1 - \mathbf{r}_2$ and $\rho_n^{(2)}(\mathbf{r}_1, \mathbf{r}_2)$ is the state-dependent two-body density matrix defined as follows

$$\rho_n^{(2)}(\mathbf{r}_1, \mathbf{r}_2) = \int \prod_{j=3}^A d\mathbf{r}_j \psi^*(\mathbf{r}_1, \dots, \mathbf{r}_A) \hat{O}_{12}^{(n)} \psi(\mathbf{r}_1, \dots, \mathbf{r}_A), \quad (5)$$

which was evaluated within the cluster expansion

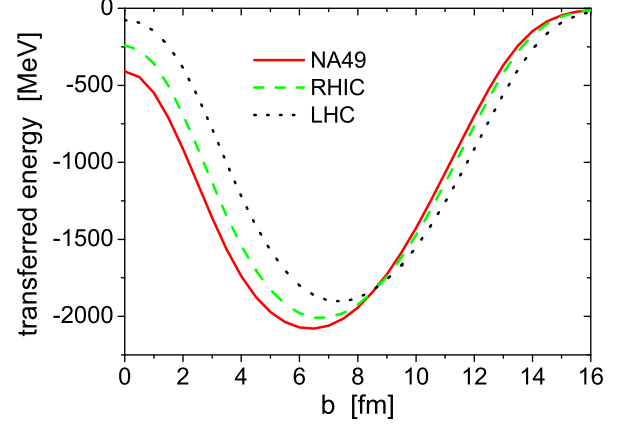


FIG. 5: (Color Online) Transferred energy in $Pb - Pb$ collisions due to the only potential energy transfer. The values of the Glauber parameters correspond to NA49 (*solid line*), RHIC (*dashed line*) and LHC (*dotted line*) energies.

method, and $\hat{O}_{12}^{(n)}$ are the operators

$$\hat{O}_{12}^{(n)} \in \left\{ \hat{1}, \boldsymbol{\sigma}_1 \cdot \boldsymbol{\sigma}_2, \hat{S}_{12} \right\} \otimes \left\{ \hat{1}, \boldsymbol{\tau}_1 \cdot \boldsymbol{\tau}_2 \right\}, \quad (6)$$

acting between particles 1 and 2 present in both the nucleon-nucleon potential and the ground state wave function, so that Eq. (1) reads

$$\begin{aligned} \psi_0(\mathbf{r}_1, \dots, \mathbf{r}_A) &= \prod_{i < j}^A \hat{f}(r_{ij}) \phi_0(\mathbf{r}_1, \dots, \mathbf{r}_A) = \\ &= \prod_{i < j}^A \sum_{n=1}^6 f^{(n)}(r_{ij}) \hat{O}_{12}^{(n)} \phi_0(\mathbf{r}_1, \dots, \mathbf{r}_A), \end{aligned} \quad (7)$$

The two-body density appearing in Eq. (4) can be easily splitted, within the cluster expansion as well as in the MC calculation, into the contributions due to proton-proton, proton-neutron and neutron-neutron pairs:

$$\begin{aligned} \rho_n^{(2)}(\mathbf{r}_1, \mathbf{r}_2) &= \\ &= \rho_{pp}^{(2,n)}(\mathbf{r}_1, \mathbf{r}_2) + \rho_{pn}^{(2,n)}(\mathbf{r}_1, \mathbf{r}_2) + \rho_{nn}^{(2,n)}(\mathbf{r}_1, \mathbf{r}_2). \end{aligned} \quad (8)$$

The potential energy can thus be splitted into the corresponding pp and pn contributions (pp and nn contributions are identical since the same single particle orbitals have been used both for protons and neutrons states). Calculations show that for *central* correlations (obviously, the total result in this case has a wrong absolute value), the individual contributions for PP and PN pairs are exactly proportional to the number of PP pairs, 23%, and PN pairs, 53%, respectively. In the case of full correlation instead, this proportionality does not hold anymore; the PP contribution represent the 8% of the total and the PN the 83% of the total; if we translate this to the contributions of isospin 0 and 1 pairs, we obtain a ratio of 74% for $I = 0$ and 26% for $I = 1$.

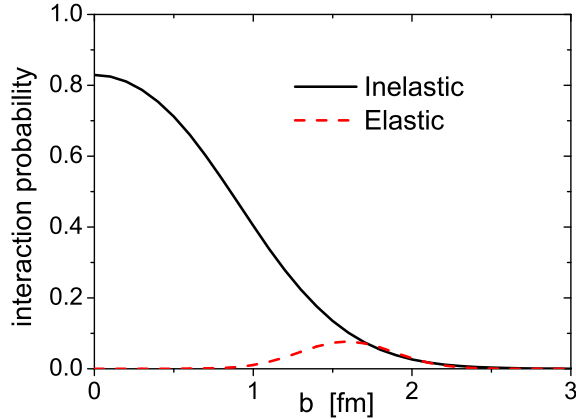


FIG. 6: (Color Online) Comparison between the probability of inelastic interaction $P_{in}(b)$ (solid line) of Eq. (3) and the elastic one $P_{el}(b)$ (dashed line), shown in Eq. (11), for values of the Glauber parameters corresponding to the experiment of Ref. [11].

We now outline how to incorporate the information presented in this Section in our Monte Carlo code. The realistic calculation of Ref. [14] provides us with the contribution to the total potential energy of a given pair of nucleons, while the corresponding calculation of total kinetic energy from momentum distributions for medium-weight nuclei, in Ref. [14], and for heavy nuclei, in Ref. [17], can be used to evaluate the total energy which is available for nucleons which escape the colliding nuclei as a result of the reaction.

For each AA event, we select spectator and interacting nucleons in both nuclei, using Eq. (3) as the interaction probability; this quantity depends upon the (nucleon pair) relative impact parameter b_{ij} . Then for a given event we can calculate the amount of potential energy which is freed by instantaneously removing the inelastically interacting nucleons: this is the amount of available energy for freeing nucleons from their bound state and to give them kinetic energy (in a sense our approximation resembles the Koltun sum rule [18]). The total potential energy of the nucleus can be calculated in terms of two-body density of the system or, more specifically, from the radial two body-density defined as follows:

$$\rho_n^{(2)}(|\mathbf{r}_{12}|) = \int d\mathbf{R} \rho_n^{(2)}\left(\mathbf{r}_1 = \mathbf{R} + \frac{\mathbf{r}_{12}}{2}, \mathbf{r}_2 = \mathbf{R} - \frac{\mathbf{r}_{12}}{2}\right). \quad (9)$$

This quantity may be easily calculated in a Monte Carlo approach by considering all the pairs and building the distribution of their relative distances; it is then straightforward to calculate the fractions of the total two-body density which are due to two spectator, two interacting, and mixed pairs. Comparing these fractions with the realistic calculations, in (small) intervals in r corresponding

to the bins used in the Monte Carlo determination of the densities, properly scaling the MC densities to the realistic calculations ones (the MC procedure is not accurate enough as far as the state-dependent radial two body density is concerned for a meaningful determination of the expectation value of the realistic, state dependent potential, whose calculation requires an accurate balance of several positive and negative parts) and rescaling to the experimental value of the binding energy of the initial nucleus, we can define the fractions $\langle V \rangle_{NN}^{SPE}$, $\langle V \rangle_{NN}^{INT}$ and $\langle V \rangle_{NN}^{MIX}$ accordingly; the procedure can also be applied to individual pn and pp pairs, along with the total ones, NN . The two-body density obtained with from the nuclear configurations we have used are presented in Fig. 3 for different nuclei; the figure shows both the results corresponding to uncorrelated and correlated configurations for the radial two-body density corresponding to the central operator, namely $\rho_{n=1}^{(2)}$ in Eqs. (5) and (9).

On the event by event basis, the fraction of potential energy is ascribed to mixed pairs of nucleons according to the procedure we outlined and becomes available for the emission of nucleons. This quantity, calculated in our model, is shown in Fig. 5 for the case of collisions at the momentum 160 GeV/c per nucleon for which the most extensive high energy studies of the fragmentation were performed; we have plotted the potential energy due to the disrupted pairs and the same (negative) quantity plus the (positive) kinetic energy due to the emission of high-momentum nucleons. Fig. 5 also shows the dependence of the transferred energy as a function of the impact parameter. We show in Fig. 6 the dependence of the transferred energy calculation upon the Glauber parameters; calculations were performed for values corresponding to NA49, RHIC and LHC energies. One can see that for average impact parameters the energy dependence is rather weak. At the same time for small impact parameters the energy transfer drops with energy since the chances for spectators to survive decrease due to increase of $\sigma_{tot}(NN)$, while the increase of $\sigma_{tot}(NN)$ leads to increase of the probability to interact with several nucleons at large impact parameters leading to increase of the energy transfer at large $b \geq 10$ fm.

The details of our model for the description of emission of nucleons are given in the next Sections.

IV. CORRELATED NUCLEONS EMISSION

We have developed a model to account for nucleon emission as a function of the solid angle $d\Omega = d(\cos\theta)d\phi$ from one of the colliding nuclei in a $^{208}\text{Pb} - ^{208}\text{Pb}$ collision. For given impact parameter b , we calculate the interaction between individual nucleons with Glauber multiple scattering theory as described in Sect. I and classify the different pairs of the nucleus as described in Sect. III. Then, from the *mixed* pairs, *i.e.* those pairs in which one of the nucleons is a spectator and the second is an interacting one, we select the *active* nucleons

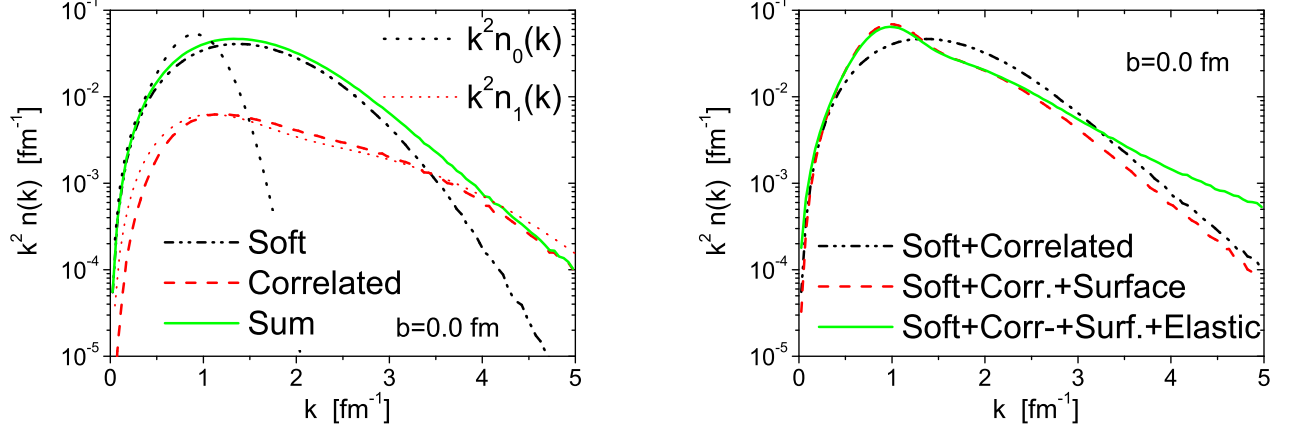


FIG. 7: (Color Online) The momentum distributions $k^2 n(k)$ of emitted nucleons in $Pb - Pb$ collisions at $P_{Lab} = 160$ GeV, calculated within our model at $b = 0$ within different approximations. *Left*: check of the input momentum distributions $n_0(k)$ and $n_1(k)$ against the MC output with no elastic scattering and no soft nucleons from the surface taken into account; the high-momentum tail of $n_1(k)$ is well reproduced. *Right*: the total momentum distributions from MC within various approximations. The normalization of each curve is set to the actual number N of nucleons falling into the corresponding definition, according to $4\pi \int dk k^2 n(k) = N$.

on the basis of the ratio between the potential energy due to the selected nucleon and the average potential energy per nucleon $\langle V \rangle_N = \epsilon - \langle T \rangle_N$ being larger than unity. Here ϵ is the (experimental) binding energy per nucleon and $\langle T \rangle_N$ the kinetic energy per nucleon calculated from the many-body parametrization of $n(k)$ of Ref. [17]. Eventually, we consider as *correlated* 25% of these active nucleons, according to the current models for the fraction of correlated nucleons in heavy nuclei and we choose, among the active ones, those nucleons which are at smaller distances from one of their interacting partners. Thus, we assign a random momentum vector with modulus given by the probability distribution $n_1(k)$, which is the correlated, high momentum tail of the momentum distribution from Ref. [17]. The correlated nucleons are then propagated through the residual system and their probability of absorption evaluated making use of data on NN elastic scattering data; we consider as absorbed those nucleons that after an elastic scattering off one of the spectator nucleons, still have a momentum larger than 250 MeV/c, the typical momentum scale of SRCs, as described below. When a nucleon is emitted, its kinetic energy will be subtracted to the available energy for the emission of soft nucleons through evaporation in the second stage.

V. ELASTIC SCATTERING

In addition to the spectators which underwent inelastic scattering, there are (primary) nucleons which scattered elastically. We model the probability of high-energy

nucleon-nucleon elastic scattering $P_{el}(b)$ in the following way. It must obey the sum rule

$$\int db P_{el}(b) = \sigma_{NN}^{el} \quad (10)$$

(at NA49 energy we have $\sigma_{NN}^{el} = 5.72$ mb), it must be a function of $b = b_{ij} = |\mathbf{b}_i - \mathbf{b}_j|$ and vanish when $P_{in}(b)$ does. We use

$$P_{el}(b) = 0.077 e^{-5.7(b-1.59)^2} \quad (11)$$

which is compared with $P_{in}(b)$ of Eq. (3) in Fig. 6.

As far as the elastic scattering in the final state is concerned, we can determine the scattering angle as follows. The target nucleon has momentum $k = \sqrt{k_t^2 + k_3^2}$ (distributed according to $n_1(k)$); the scattered nucleon has momentum $p = \sqrt{p_t^2 + p_3^2}$; the four momentum transfer q can be assumed to have $q_0 = q_3$ since we are at high energies so that $t = q^2 = q_0^2 - q_t^2 - q_3^2 = -q_t^2$; t can be randomly generated using the elastic scattering amplitude

$$\frac{d\sigma_{NN}^{el}}{dt} = \frac{\sigma_{NN}^{tot\ 2}}{16\pi} e^{Bt} \quad (12)$$

from which we determine q_t and $p_t = q_t + k_t$; then

$$\alpha = 1 + \frac{k_3}{m} = \frac{\sqrt{p_t^2 + p_3^2 + m^2} - p_3}{m} \quad (13)$$

gives

$$p_3 = \frac{p_t^2 + m^2 - m^2 \alpha^2}{2m\alpha} \quad (14)$$

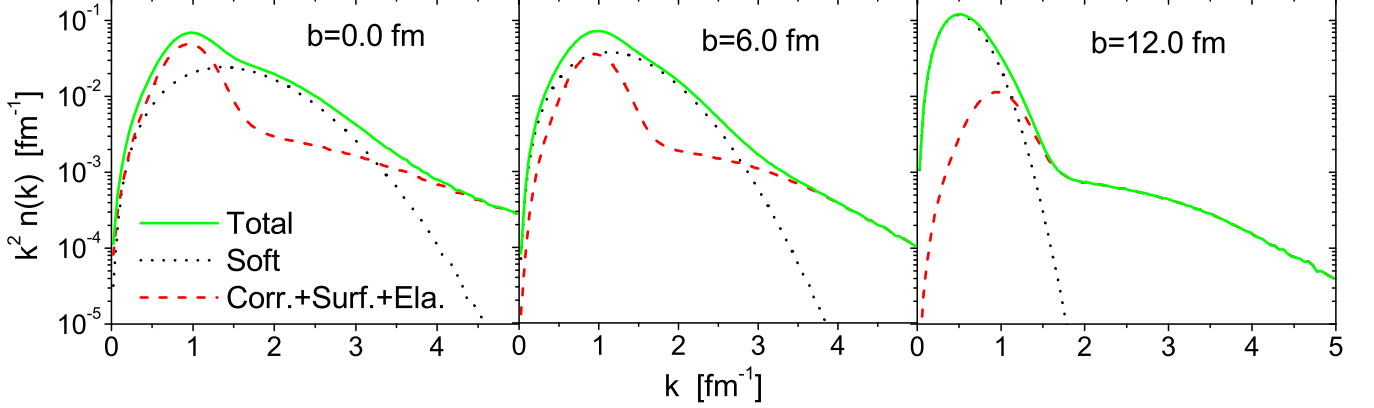


FIG. 8: (Color Online) The momentum distributions $k^2 n(k)$ of emitted nucleons in $Pb - Pb$ collisions at $P_{Lab} = 160$ GeV, calculated within our full model, where soft, surface, both low-momentum and correlated, and elastically scattered nucleons are taken into account. The panels show the soft and high momentum contributions to the total momentum distribution, plotted for $b = 0$, $b = 6$ and $b = 12$ fm: note that for central collisions the shape of the momentum distribution is very similar to the input nucleon $n(k)$ in nuclei, while when b increases the dominant contribution is the soft part.

so that the scattering angle θ is

$$\tan \theta = p_t/p_3. \quad (15)$$

We can evaluate the attenuation of both the spectators and elastically scattered nucleons using $d\sigma_{NN}^{el}/dT$ of Ref. [19] given as a function of incident proton kinetic energy $T = T_{lab}$ (tabulated for $40 \text{ MeV} < T < 600 \text{ MeV}$) and center of mass scattering angle θ_{CM} (tabulated for $0 < \theta_{CM} < \pi$). We will consider as thermalized those nucleons which as a consequence of elastic scattering loose $T_{min} = \sqrt{k_{min}^2 + m^2} - m$ kinetic energy, where $k_{min} = 250 \text{ MeV}$. First, we consider as interacting elastically two nucleons whose transverse separation (with respect to the direction of propagation of the nucleon under investigation) is $b_{ij} < \sqrt{\sigma_{NN}^{el}/\pi}$ with σ_{NN}^{el} evaluated at the corresponding incident momentum, taken from the tabulated values of Ref. [19]. If $k = k_{lab} = \sqrt{(T - m)^2 + m^2}$ is the emitted nucleon momentum in the lab hitting a spectator nucleon at rest which recoils with kinetic energy T_4 we have

$$t = -2mT_4 = -2p^2(1 - \cos \theta_{CM}) \quad (16)$$

where $p = k_{CM} = \sqrt{\frac{1}{2}m\sqrt{k^2 + m^2} - \frac{1}{2}m^2}$ is the incident nucleon momentum in the CM. Then, the probability of losing more than $T_{min} = T_4 - T$ is given by

$$\int_0^T dT \frac{d\sigma_{NN}^{el}(T, \theta_{CM})}{dT} / \int_0^\infty dT \frac{d\sigma_{NN}^{el}(T, \theta_{CM})}{dT}. \quad (17)$$

Since we have tables for $40 \text{ MeV} < T < 600 \text{ MeV}$, the

integration limits in Eq. (17) become

$$\int_{40}^{Min(T, 600)} dT \frac{d\sigma_{NN}^{el}(T, \theta_{CM})}{dT} / \int_{40}^{600} dT \frac{d\sigma_{NN}^{el}(T, \theta_{CM})}{dT} \quad (18)$$

and we consider as lost (absorbed in the nuclear medium) those nucleons with $T < 40 \text{ MeV}$ and non interacting those with $T > 600 \text{ MeV}$. In Eq. (18) we use $d\sigma_{pp}^{el}$ both for pp and nn scatterings, and $d\sigma_{pn}^{el}$ for pn and np . The same procedure has been used to calculate the attenuation of the primary elastically scattered nucleons, where the incident momentum k is replaced by p given in Eq. (15) and their kinetic energy will be added to the available energy in case of absorption by the spectator system.

VI. MOMENTUM DISTRIBUTIONS

In our model, there are different mechanisms for emitting nucleons as a consequence of the AA interaction. There is one standard mechanisms to describe spectator emission from fragmentation, which is due to excitation of the residual system and subsequent evaporation of nucleons with the exponential probability for the emitted nucleon kinetic energy $T_n = p_n^2/2m$ [20–22]:

$$P(T_n) = e^{-T_n/T_F}, \quad (19)$$

where T_F is typically assumed to be the Fermi kinetic energy. We can estimate the kinetic energy T_0 for a given value of the impact parameter in the following way. We have calculated the energy released by disruption of nucleon-nucleon pairs in Section III. This energy must be distributed among the evaporating nucleons according

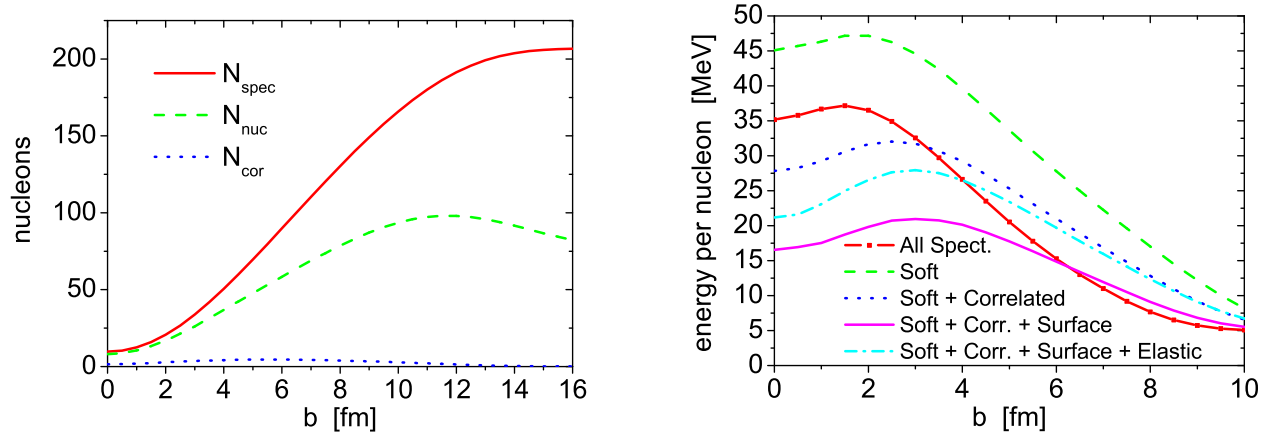


FIG. 9: (Color Online) *Top*: Spectators in a $Pb - Pb$ collision within Glauber model, at NA49 energy ($P_{Lab} = 160 \text{ GeV } A$). The total number of spectators N_{spec} , unbound nucleons N_{nuc} , and high-momentum nucleons N_{corr} are shown. Data from the NA49 experiment [11] was used to determine the spectators/emitted nucleons ratio. *Bottom*: The kinetic energy per emitted soft nucleon as calculated in our model within the approximations described in Section VI, where the available energy is shared by: *red solid*: all spectator nucleons; *green dashed*: only soft, evaporating nucleons; *blue dotted*: evaporation and correlated nucleons; *magenta dotted*: evaporation, correlated nucleons and soft nucleons from the inner surface; *cyan dot-dashed*: evaporation, correlated nucleons, soft nucleons from the inner surface and primary elastically scattered nucleons which may increase the available energy.

to the following energy balance equation:

$$N_{nucl}(T_n + \epsilon) = -V' - \epsilon N_{corr} \quad (20)$$

where N_{nucl} is the number of emitted soft nucleons, N_{corr} the number of emitted correlated nucleons, ϵ the binding energy per nucleon and $V' = V(1 + \epsilon / \langle V \rangle_n) < 0$ the energy released, as described in Section III, corrected for binding effects of the removed nucleons. Eq. (20) states that the amount of energy ϵ must be spent for each of the emitted nucleons, and the available energy is provided by the calculated potential energy; note that N_{nucl} , N_{corr} and V depend on the AA impact parameter b , and so does the energy per emitted soft nucleon T_0 to be used in Eq. (19) in place of T_F . The energy balance expressed by Eq. (20) must be corrected for a few additional effects. Nucleons emitted by evaporation are not the totality of spectator nucleons, a large number of them being present in compounds (deuterons, tritons, 3He , alphas, and heavier fragments) which carry little kinetic energy as compared with free nucleons. For this reason the number N_{nucl} does not coincide with the number of spectators but it is rather replaced in Eq. (20) by $N_{nucl} + K N_{frag}$ where N_{frag} is the total number of nucleons present in compound fragments and K a factor which effectively takes into account the fact that these nucleons carry less energy than free nucleons. This factor can be determined from the measurements of Refs. [12] and [11]. We determined from the data what fraction of nucleons are in the form of fragments and, for the given kind of fragments, what is the kinetic energy as compared to the one of observed protons, and com-

binning this information we found the factor to be about $K = 0.3$ with no additional assumptions. Other effects to be accounted for in Eq. (20) are especially relevant for the determination of the momentum distributions of the emerging nucleon and are the following. The number of correlated nucleons N_{corr} determined as described in Section IV is only a fraction of the active nucleons whose "broken links" with the removed ones produce a large fraction of available energy; the remaining of these nucleons, which are located on the inner surface resulting from the removal of a certain number of interacting nucleons, must be considered as escaping the system as well, but with a momentum distribution given by the low momentum part $n_0(k)$ of the model of Ref. [17]; this assumption is reasonable since we assume the active nucleons to be emitted with the same momenta they had in the nucleus, but is somewhat arbitrary.

Note that the production of the nucleons from the correlations has forward - backward asymmetry which for moderate momenta is given by the flux factor $(1 + k_3/m_N)$ where k_3 is the longitudinal component of the nucleon momentum in its rest frame. So more nucleons are emitted forward (along the beam direction of the projectile) in the rest frame of a nucleus. In this paper to simplify the discussion we consider quantities symmetrized over $k_3 \rightarrow -k_3$.

The last kind of nucleons we want to take into account are those emerging as recoiling from primary elastic scatterings. In a similar way to what we described for the propagation of correlated nucleons, we assign momenta to the hit nucleons according to the full $n(k) =$

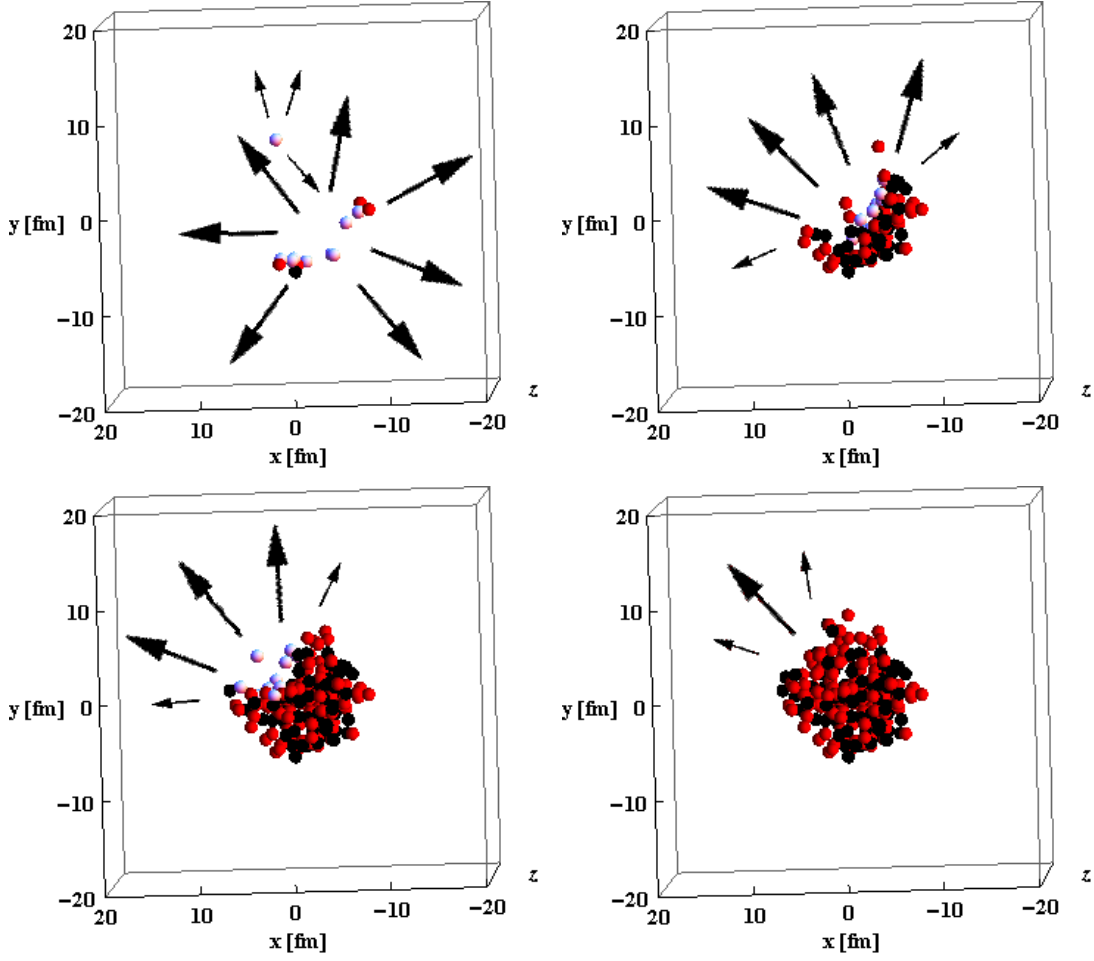


FIG. 10: (Color Online) Sketch of the asymmetry of emission of high-momentum, correlated nucleons defined in Eq. (21) and quantitatively evaluated in Fig. 11, in Pb-Pb collision; the preferred direction of emission is shown with arrows as a function of the impact parameter which is oriented as in Fig. 1 and its values are $b=1, 5, 10$ and 15 fm moving from left to right, top to bottom through the different panels.

$n_0(k) + n_1(k)$ and using the available NN elastic scattering data we decide if the nucleon is absorbed, its energy going into additional heating of the spectator system, or emitted with its recoiling momentum, to be collected in the final momentum distribution.

Results for the calculated momentum distributions are shown in Figs. 7 and 8. The curves shown in the figures correspond to the inclusion of the different effects we have described in this Section. In these figures and in the following ones, the curves labeled with *soft* correspond to the energy per emitted nucleon obtained dividing the total potential energy by the number of expected free nucleons; the other curves are obtained by modifying these two quantities by i) the energy going into kinetic energy of emitted particles and the kinetic energy of absorbed particles going into additional available energy and ii) the number of nucleons emitted in the first stage from the surface close the the interaction - these are either high momentum or soft nucleons, whose number is subtracted from the number of free nucleons. *Soft +*

correlations correspond to the inclusion high momentum nucleons emitted from the surface; *soft + correlations + surface* correspond to the inclusion high momentum as well as soft nucleons from the surface; *soft + correlations + surface + elastic* correspond to all the above, plus the contributions from primary elastically scattered nucleons, which may be absorbed by the spectator system. The energy per soft nucleon is shown in Fig. 9 within the various approximations we have described.

We eventually would like to comment on Anderson data [12], where momentum distributions of detected nucleons were explicitly measured. Nonetheless, a direct comparison with our results may not be trivial. They have compared the observed momentum distribution with the theoretical momentum distribution in nuclei, which is not consistent with the observation that i) most of the nucleons are emitted by the evaporation mechanism, whose distribution is given by Eq. (19) and it is expected to be rather different from the momentum distribution of nucleons inside the nucleus; ii) the ob-

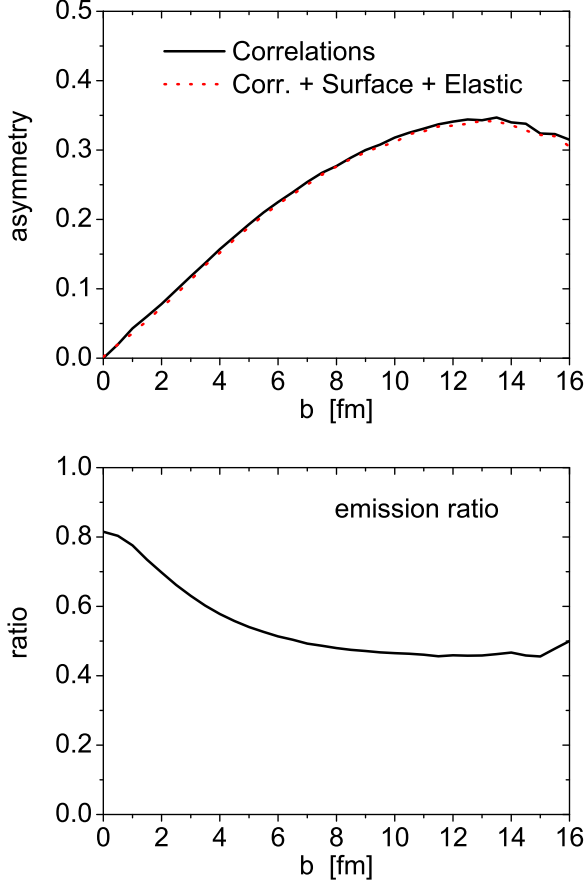


FIG. 11: *Top*: the asymmetry defined in Eq. (21) within the approximations described in Section VI; in the three cases, the curves show little difference. *Bottom*: the fraction of emitted high-momentum nucleons which survive after scattering off the spectator system, disregarding any angular dependence.

served momentum distribution depends upon the transferred energy in the process of removing one nucleon while the momentum distribution is the integral of the spectral function over all the removal energy range; a calculation of the effects of the integration of the spectral function on a limited region of energy may be found in Ref. [23]; iii) we suggest that only the high momentum part of the observed momentum distribution can be compared with the nucleon momentum distribution in nuclei $n(k)$, since it is due to direct emission of correlated nucleons whose momentum may be distorted by propagation through the spectator system but will be similar to the original $n(k)$. Moreover, the high momentum region of the observed momentum distribution is also affected by primary elastically scattered nucleons, which must be taken into account. Anderson data observed a change in slope of the momentum distribution of protons which may be due to high momentum, correlated nucleons.

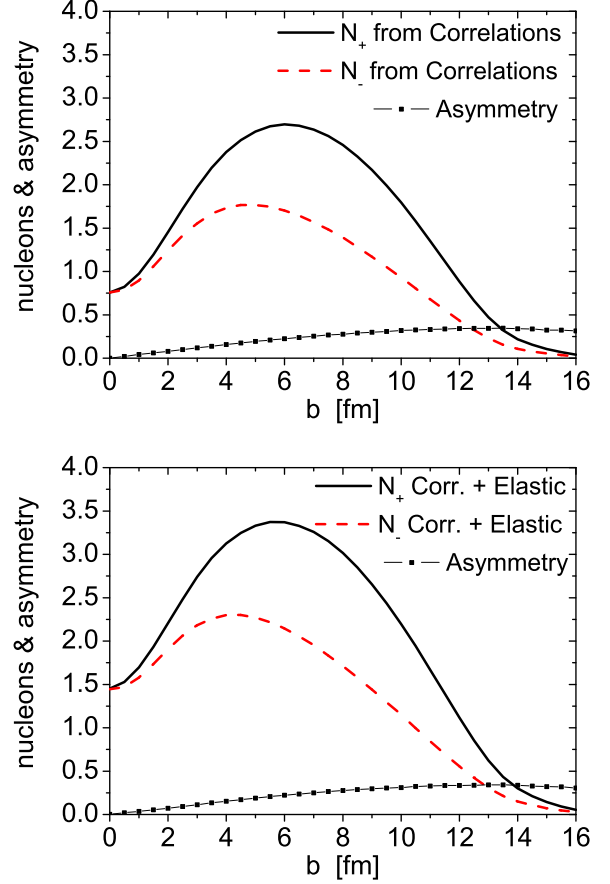


FIG. 12: The number of high-momentum nucleons emitted in the emisphere containing the projectile (N_+ ; solid curve) and in the opposite one (N_- ; dashed curve); the line + symbol curve represent the asymmetry defined in Eq. (21). The different quantities have been calculated our model within the approximations described in Section VI. *Top*: only correlated nucleons; *bottom*: correlated nucleons with inclusion of primary elastically scattered nucleons.

VII. ANGULAR DEPENDENCE OF EMITTED HIGH-MOMENTUM NUCLEONS

One of the aims of this work is to estimate the asymmetry of high-momentum nucleons emerging from the AA collision. These nucleons are generated on the inner surface left after the fast propagation of the projectile nucleus; we define N_+ to be the number of nucleons ending up in the emisphere oriented towards free space and N_- its analogue in the opposite emisphere. We expect that the few nucleons surviving in a central collision will find little or no matter to propagate through in any direction, resulting in $A(0) = 0$. The situation is depicted in Fig. 10, for different impact parameters ranging from $b = 1$ fm (top left panel) to $b = 15$ fm (bottom right panel). In the first case of almost central collision, few nucleons are left,

far from each other and free to propagate. For increasing b , it can be seen how an asymmetry arise in the rest frame of the target nucleus, since nucleons are produced with random momentum direction and they can end up propagating into free space or through the spectator system which prevents emitted nucleons to propagate freely. We can define the impact-parameter dependent asymmetry as follows:

$$A(b) = \frac{N_+ - N_-}{N_+ + N_-} \quad (21)$$

For large impact parameter, the asymmetry of Eq. (21) should approach the value given by taking $N_- \simeq 0.5N_+$, which is the fraction of nucleons surviving scatterings through the spectator matter at large impact parameters, which would give $A(b) \simeq 0.3$. The calculations of $A(b)$ performed within our model are shown in Figs. 11, 12 and confirm these expectations.

This evaluation of the asymmetry $A(b)$ could be used in one given observed event by matching on the reaction plane the asymmetry of emitted nucleon produced by one of the spectator system with an asymmetry on the opposite direction produced by the other nucleus. This would allow to resolve the ambiguity in the sign of the impact parameter b . It could be used to see whether production of hadrons at more central rapidities depends (probably rather weakly) on the direction of b .

VIII. COMPARISON WITH THE ABRASION-ABLATION MODEL

In this section we compare our novel approach for the calculation of the excitation energy of the spectator system with the one employed in Ref. [1]. In the cited Reference, the authors use the abrasion-ablation model for hadronic interactions and the relativistic electromagnetic dissociation model for electromagnetic interactions of relativistic heavy ions to describe data of charge-changing cross section in Pb-A collisions. In particular they address the question of how to estimate the excitation energy of a nuclear system formed by sudden removal of several nucleons, which is also one of the main aims of the present work, and describe the decay of excited nuclear systems within the statistical multi-fragmentation model. The abrasion model describes participant and spectator nucleons with participants originating from the overlapping parts of the colliding nuclei, while their non-overlapping parts are treated as spectators which represent excited remnants of the initial nuclei which undergo secondary decay by statistical evaporation and fission models in the so-called ablation model.

The NN interaction probability in Ref. [1] is defined through (uncorrelated) nuclear thickness functions, while in our approach correlations are taken into account automatically by using improved configurations from Ref. [7]. Then, the main difference consists in the estimate of the spectator system (prefragment, in their language)

excitation energy. We use similar values of NN cross sections. The authors of Ref. [1] describe excitation energy by the abrasion model, which basically evaluate the energy due to a hole in the uncorrelated ground state of the initial nucleus, while we use the realistic calculation of Section III; moreover, in Ref. [1] it is explicitly mentioned that the procedure is not well defined for a large number of removed nucleons and that their method of calculating excitation energies of prefragments via the hole state densities should only be considered as a model assumption. A comparison with other approaches was also done in Ref. [1], finding for the excitation energy per nucleon a value of $\simeq 40$ MeV using the ablation model, and $\simeq 27$ MeV using a more refined formula, the latter estimate being confirmed by data; we note that the value of $\simeq 27$ MeV is in good agreement with our findings of Fig. 9, where this value is just about our estimate for $b \simeq 3 - 4$ fm; we believe that one of the important improvement of our approach is precisely the possibility of giving an impact-parameter dependent estimate of the excitation energy, which was untouched by any of the previous approaches. As a last remark, let us stress that in Ref. [1] it was mentioned that their model should be complemented with FSI, which we take into account in our estimate of the energy per nucleon, and the additional energy brought in by elastically scattered primary nucleons subsequently absorbed by the spectator system, which we also considered.

IX. CONCLUSIONS

We have demonstrated that the underlying dynamics of the process of the nucleus fragmentation in high energy nucleus-nucleus collisions is strongly related to the presence of the short-range correlations in nuclei. We predict a number of new phenomena which could be tested in the current and forthcoming heavy ion experiments including the dependence of the momentum spectrum on the impact parameter strong asymmetry of the emission nucleons along the b direction. Such an asymmetry as well as other predicted effects maybe of use for more detailed analyses of dynamics of the heavy ion collisions. In particular, it would allow one to investigate whether similar asymmetry is present for the hadrons produced in AA collisions away from zero center of mass rapidity. We also predict a close connection of the spectrum of nucleons in the central collisions and momentum distribution in the nuclei. We are now in the process of implementing the discussed effects in a complete MC event generator of AA collisions and results will be presented elsewhere [24].

X. ACKNOWLEDGEMENTS

We thank G. Bertsch, L. Frankfurt, I. N. Mishustin and I. A. Pshenichnov for very useful discussions. This work

is supported by DOE grant under contract DE-FG02-93ER40771. M.A. thanks the HPC-Europa2 Consortium (project number: 228398), with the support of the EC -

Research Infrastructure Action of the FP7 - and EPCC, Edinburgh for the use of computing facilities.

-
- [1] C. Scheidenberger *et al.*, Phys. Rev. C **70**, 014902 (2004).
 - [2] R. Subedi *et al.*, Science **320**, 1476 (2008)
 - [3] R. Shneor *et al.* [Jefferson Lab Hall A Collaboration], Phys. Rev. Lett. **99**, 072501 (2007)
 - [4] E. Piasetzky, M. Sargsian, L. Frankfurt, M. Strikman and J. W. Watson, Phys. Rev. Lett. **97**, 162504 (2006)
 - [5] A. Tang *et al.*, Phys. Rev. Lett. **90**, 042301 (2003)
 - [6] L. Frankfurt, M. Sargsian and M. Strikman, Int. J. Mod. Phys. A **23**, 2991 (2008)
 - [7] M. Alvioli, H. J. Drescher and M. Strikman, Phys. Lett. B **680**, 225 (2009)
 - [8] W. Broniowski, M. Chojnacki and L. Obara, Phys. Rev. C **80** (2009) 051902
 - [9] W. Broniowski and M. Rybczynski, Phys. Rev. C **81**, 064909 (2010)
 - [10] <http://www.phys.psu.edu/~malvioli/eventgenerator>
 - [11] H. Appelhauser *et al.*, Eur. Phys. J. A **2**, 383 (1998).
 - [12] L. Anderson *et al.*, Phys. Rev. C **28**, 1246 (1983).
 - [13] J. Aichelin, Phys. Rept. **202**, 233 (1991).
 - [14] M. Alvioli, C. Ciofi degli Atti and H. Morita, Phys. Rev. C **72**, 054310 (2005)
 - [15] X. N. Wang and M. Gyulassy, Phys. Rev. D **44**, 3501 (1991).
 - [16] M. Alvioli, C. Ciofi degli Atti and H. Morita, Phys. Rev. Lett. **100**, 162503 (2008).
 - [17] C. Ciofi degli Atti and S. Simula, Phys. Rev. C **53**, 1689 (1996)
 - [18] D. S. Koltun, Phys. Rev. C **9**, 484 (1974).
 - [19] R. A. Arndt, W. J. Briscoe, I. I. Strakovsky and R. L. Workman, Phys. Rev. C **76**, 025209 (2007) and *private communication*
 - [20] M. Strikman, M. G. Tverskoy and M. J. Zhalov, Phys. Lett. B, 459 (1999).
 - [21] S. White and M. Strikman, arXiv:0910.3205 [nucl-ex].
 - [22] H. Feshbach and K. Huang, Phys. Lett. B **47**, 300 (1973).
 - [23] C. Ciofi degli Atti, E. Pace and G. Salmè, Phys. Lett. B **141**, 14 (1984)
 - [24] M. Alvioli, M. Striman, S. White, M. Vargyas, A. Ster and T. Csorgo, *in preparation*